Reduction of Underpad Stress in Thermosonic Copper Ball Bonding

A. Shah(1), M. Mayer(1), Y. Zhou(1), S. J. Hong (2), and J. T. Moon (2)
(1) Microjoining Laboratory, University of Waterloo, Waterloo, ON, N2L 3G1, CANADA.
(2) MK Electron Co. Ltd, Yongin, KOREA.
ashah011@uwaterloo.ca

Abstract

Ball bonding processes on test chips with Al metallized bonding pads are optimized with one Au and two Cu wire types, all 25 µm diameter, obtaining average shear strengths of more than 120 MPa. The process temperature is about 110 °C. The results demonstrate that ball bonds made with Cu wire show at least 15% higher shear strength than those made with Au wire. The estimated maximum shear strength c_{pk} value determined for Cu ball bonding (c_{pk} = 3.7 ± 1.2) is almost 1.5 times as large than that of the Au ball bonding process (c_{pk} = 2.3 ± 0.9), where *LSL* is 65.2 MPa. However, the ultrasound level required for Cu is approximately 1.3 times that required for Au. Consequently, about 30% higher ultrasonic forces induced to the bonding pad are measured using integrated real-time microsensors. The higher stresses increases the risk of underpad damage.

One way to reduce ultrasonic bonding stresses is by choosing the softer of the two Cu wire types, resulting in a measured ultrasonic force reduction of about 5%. A second way is to reduce the ultrasound level. While this causes the average shear strength to fall by 15%, the ultrasonic force falls by 9%. The c_{pk} value does not change significantly, suggesting that a successful Cu ball bonding operation can be run with about 0.9 times the conventionally optimized ultrasound level. The process adjusted in this way reduces the extra stress observed with Cu wire compared to that observed with Au wire by 39%. Hence, significantly lower than optimized ultrasound levels can be used in a Cu wire bonding process to obtain c_{pk} values higher than that of a comparable Au wire bonding process while reducing the risk for underpad damage.

Introduction

The continued emphasis in microelectronics on reducing manufacturing costs and improving performance is driving the development of low-cost packaging for fine pitch, high input-output devices. This has led to an increased interest towards the development of new materials for wire bonding process. Compared to Au wire, Cu wire has superior electrical and thermal conductivities. Coupled with its lower cost, it is considered a candidate to replace Au in wire bonding. Due to its higher mechanical strength, thinner and longer wires can be used, particularly for today's demands on finer pitches and smaller packages. However, since Cu is harder than Au, it requires the application of higher normal and ultrasonic forces for making strong bonds. This increases the likelihood of underpad damage such as pad peeling or silicon cratering, particularly in the case of sensitive substrates such as low-k chips. Controlling and optimizing the process settings to avoid underpad damage is therefore a major challenge towards the implementation of a robust Cu ball bonding process.

The processes used in wire bonding typically fall between two extreme process types: *ultrasound enhanced deformation* (UED) process [1] and *impact deformation* process [2, 3]. In the UED process as shown in Fig. 1 (a), a low impact force is used followed by a relatively high bond force. In such a process most of the wire deformation and bonding takes place during the ultrasonic vibrations. In the impact deformation process shown in Fig. 1 (b), an impact force which is two to three times higher than a relatively low bond force is used. Most of the wire deformation is caused by the impact force. Ultrasound is present only after impact, does not contribute to the plastic wire deformation, and solely needed for bonding. Previous studies using Au [2] and Cu [3] wires reported that impact deformation process (also called double-load bonding process) aids in reducing defects related to bonding stress (e.g. cratering).

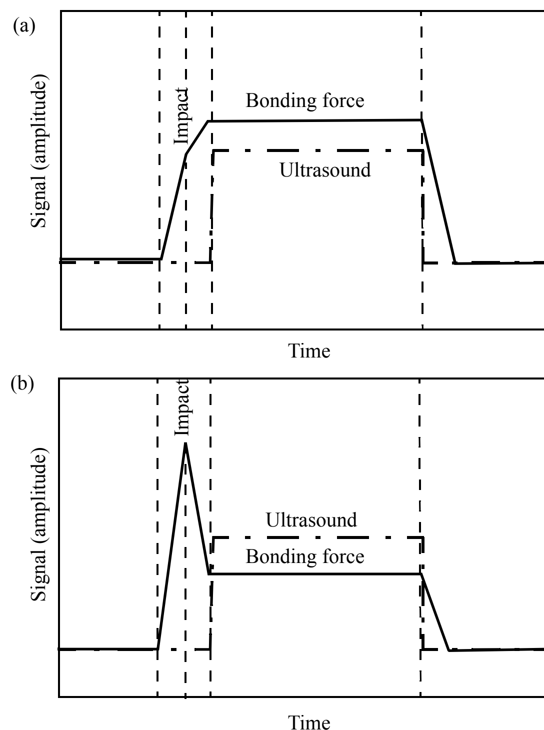

Fig. 1 Illustrations of force and ultrasound profiles used for (a) ultrasound enhanced deformation (UED) process and (b) Impact deformation process.

In this study, an accelerated method to optimize the ball bonding process parameters is used based on the impact deformation process to minimize the underpad stresses.

Experimental

The automatic ESEC 3100 wire bonder, manufactured by Oerlikon ESEC, Cham, Switzerland, is used to perform thermosonic ball bonding with a standard Au wire, a hard Cu wire (Cu-H), and a soft Cu wire (Cu-S), all 25 µm in diameter, manufactured by MK Electron Co. Ltd.,Yongin, Korea. Table 1 shows the basic mechanical properties of the three wire types. The values for vicker's hardness were measured on the wire cross-sections made perpendicular to the wire main axis. Using the deformability characterization method reported in [3], it is found that the free air ball (FAB) made with Cu-S wire is softer than that made with Cu-H wire.

Bonding is performed at a nominal heater plate temperature of 125 °C, resulting in actual chip temperature of about 110 °C. A commercial ceramics bottleneck capillary having a hole diameter of 35 µm and a chamfer diameter of 51 µm is used. During the formation of free-air balls (FABs) with the copper wires, a homogeneous mixture of 95% nitrogen and 5% hydrogen is used as a shielding gas to prevent the oxidation of the molten FAB metal during solidification. The flow rate of the shielding gas is set to 0.48 litres per min.

Optimization of processes

The wedge bonding parameters are optimized using an iterative method reported in [4], and shown in Table 2. These parameters result in symmetrical shapes without signs of fish tailing (peeling). The unit "%" is used for the ultrasonic parameter, where 1% is equivalent to a peak to peak vibration amplitude of 26.6 nm measured at the center of the transducer tip.

Next, the parameters for the electrical flame-off (EFO) process are optimized to obtain a 50 µm diameter FAB. To this end, 30 FABs are made with three different levels of EFO current (10 FABs for each current level), and fixing all other EFO parameters such as tail length to 500 µm, EFO time to 0.4 ms, and electrode to wire (E-W) distance to 300 µm. The FAB diameters are measured using an optical microscope and fitted with a second order polynomial against the EFO current. From the fitted curve, the EFO current corresponding to a 50 µm FAB is determined. An example plot visualizing this procedure is shown in Fig. 2. Table 3 shows the resulting EFO currents. Using this optimized EFO current, sample FABs are made and the diameters are verified to be 50 ± 0.5 µm.

An impact force which is nominally three times as high as the subsequent bond force is used. Ultrasound is present only after impact. The nominal parameters are given in Table 4 . To verify the nominal impact to bond force ratio, the actual forces applied by the machine are recorded in real-time by the proximity sensor attached to the wire clamp of the bonder [4]. Example force profiles are shown in Figs. 3 (a), (b), and (c). It is observed that the actual impact to bond force ratio is about 2.9.

The impact force values were adjusted such that the ball geometries were the same with each of the three wires with a target bonded ball diameter measured at the capillary imprint (BDC) of 60 µm. The nominal bonding force is then calculated to maintain the ratio described before.

The bonding time parameter describes the duration of ultrasound. Relatively long times of 25 ms were chosen to

Table 1: Wire Properties

Property	Au	Cu-H	Cu-S
Breaking load [gf]	10.0	12.6	10.1
Elongation [%]	2.8	14.9	11.2
Vicker's hardness	50.0	57.8	55.5

Table 2: Wedge bond parameters

	Au	Cu-H	Cu-S
Impact force [mN]	700	800	700
Bond force [mN]	350	500	700
Ultrasound [%]	65	75	75
Bond time [ms]	25	65	65
Pre-ultrasound, off at impact [%]	0	30	30

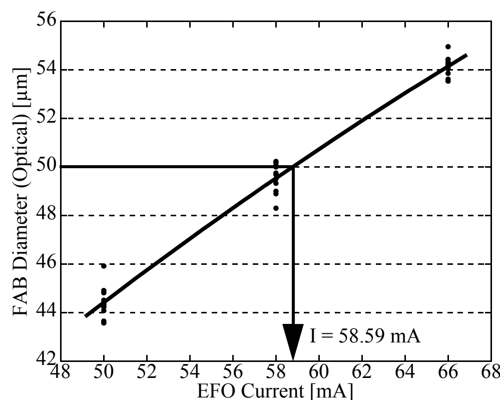

Fig. 2 FAB diameter vs. EFO current for Au wire. Thick solid line is second order polynomial fit.

Table 3: EFO currents to obtain 50 µm diameter FABs

	Au	Cu-H	Cu-S
Current [mA]	58.59	81.63	83.25

cover eventual process mechanisms occurring later during bonding and made visible by microsensor signals. The chips with Al metallized bond pads used for the tests were supplied by Oerlikon ESEC, Cham, Switzerland. An example is shown in Fig. 4 mounted on a PLCC44 lead frame. On each chip, ball bonding is performed by varying the ultrasound from the minimum ultrasound required to avoid ball non-stick on pad (NSOP), in steps to high ultrasound when the ball is heavily deformed. For levels lower than the ultrasound ranges specified in Table 4, NSOPs are observed.

Table 4: Ball bonding parameters

	Au	Cu-H	Cu-S
Impact force [mN]	800	1200	1200
Bond force [mN]	266	400	400
Bond time [ms]	25	25	25
Ultrasound [%]	25-70	50-86	50-86

A set of 14 bonds using different ultrasound values for each is made per chip, repeated on ten chips. Example micrographs of typical optimized ball bonds with Au, Cu-H, and Cu-S wires are shown in Figs. 5 (a), (b), and (c), respectively. BDC and ball height (BH) values are measured at the capillary imprint using an optical microscope. Then the balls are sheared, and the shear force (SF) is recorded. Example micrographs of the pad morphology after shearing the ball bonds with Au, Cu-H, and Cu-S ball bonds are shown in Figs. 6 (a), (b), and (c), respectively. It is observed that during the shearing of Cu ball bonds, fracture occurred at the Cu-Al bond interface, while for Au ball bonds, failure occurred in the Au ball.

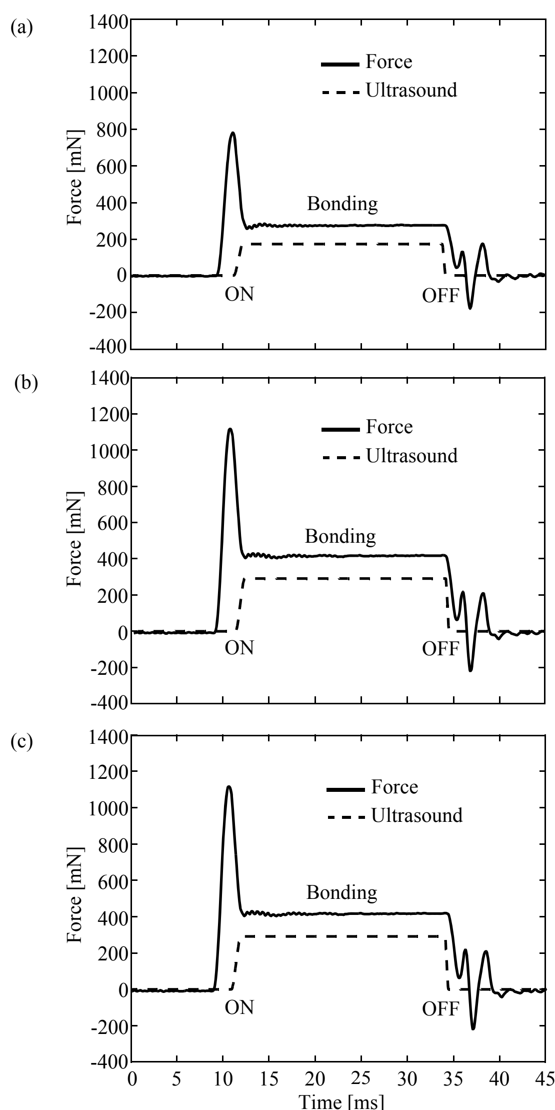

Fig. 3 Example measured force profiles of ball bonding process with (a) Au, (b) Cu-H and Cu-S wires.

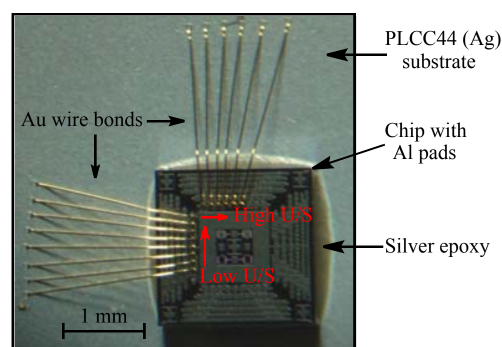

Fig. 4 Test chip used for ball bonding process optimization.

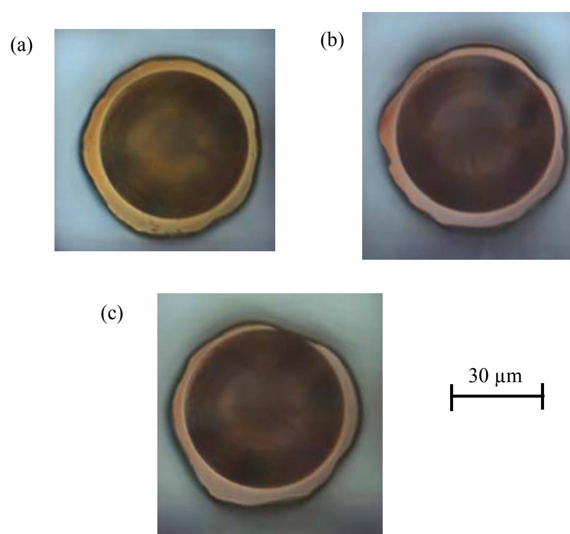

Fig. 5 Example micrographs of optimized ball bonds made with (a) Au, (b) Cu-H, and (c) Cu-S wires.

The shear strength (SS) of the ball bond is defined as the shear force divided by the cross-sectional area A, where $A = \pi\,(\mathrm{BDC}/2)^2$. The variations of BDC, BH, and SS as a function of ultrasound are plotted in Figs. 7, 8 and 9, for the processes with Au, Cu-H, and Cu-S wires, respectively. The optimum ultrasound levels are selected at the point (indicated by arrows in the figures) when a sharp increase in BDC and decrease in BH is observed. This is the maximum ultrasound at which there is no UED, i.e., the ball deformation is due to the normal impact force alone. The values for the processes with Au, Cu-H, and Cu-S wires are 51%, 70%, and 66%, respectively, as indicated by the arrows in Fig. 7.

Evaluation of processes

It is observed that the ball bonds made with Cu wires have higher shear strengths than those made with Au wire. This is consistent with the findings reported in [5]. One of the reasons for this higher shear strength is possibly the higher ultrasound stress supported by Cu without yielding. If the ultrasound stress induced to the ball is larger than the yield strength, an additional UED occurs, and the bonded ball dimensions are out of specifications. Since, Cu has a tensile strength of about 210 MPa which is almost double that of Au, 120 MPa [6], higher ultrasound levels can be used without UED, resulting in stronger bonds.

To quantify the process capability (i.e. the ability of the process to produce output within specification limits), the c_{pk} value is calculated using Eqn. (1) [7].

$$c_{pk} = \frac{\mu - LSL}{3\sigma} \tag{1}$$

where μ, LSL, and σ are the average, lower specification limit, and standard deviation of the ball bond shear strength, respectively. From the EIA/JEDEC Standard 22-B116 [8], LSL is defined to be 65.2 MPa.

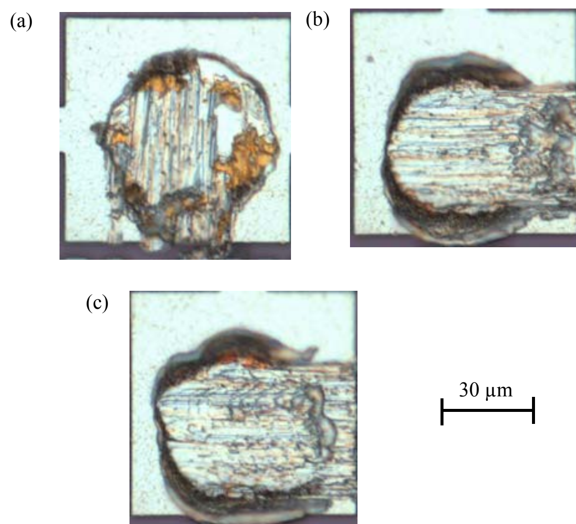

Fig. 6 Example micrographs of pad morphology after shearing the ball bonds with (a) Au, (b) Cu-H, and (c) Cu-S wires.

The c_{pk} values are determined for various ultrasound levels for each of the three wire types and plotted in Figs. 10 (a), (b), and (c), respectively, together with parabolic curve fits. The fits are used to estimate maximum c_{pk} values at the optimized ultrasound parameter. These are found to be 2.3 ± 0.9, 3.3 ± 1.4, and 3.7 ± 1.2 for Au, Cu-H, and Cu-S wires respectively.

The maximum shear strength c_{pk} value determined for Cu ball bonding is approximately 1.5 times as large than that of the Au ball bonding process. However, the ultrasound level required for Cu is approximately 30-37% higher than that required for Au. The higher ultrasound results in higher force induced to the pad during the bonding process which increases the risk of underpad damage.

Ultrasound reduction

One way to reduce this stress is to reduce the ultrasound level during the process. A trade-off is expected between such a parameter reduction and achieving a high bond quality.

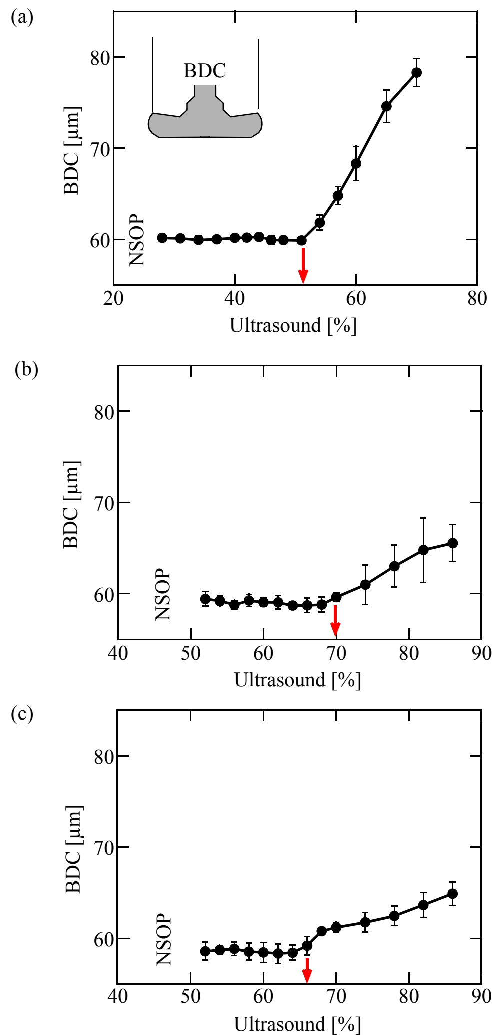

Fig. 7 Ball bond diameter (BDC) vs. ultrasound for (a) Au, (b) Cu-H and (c) Cu-S wire process.

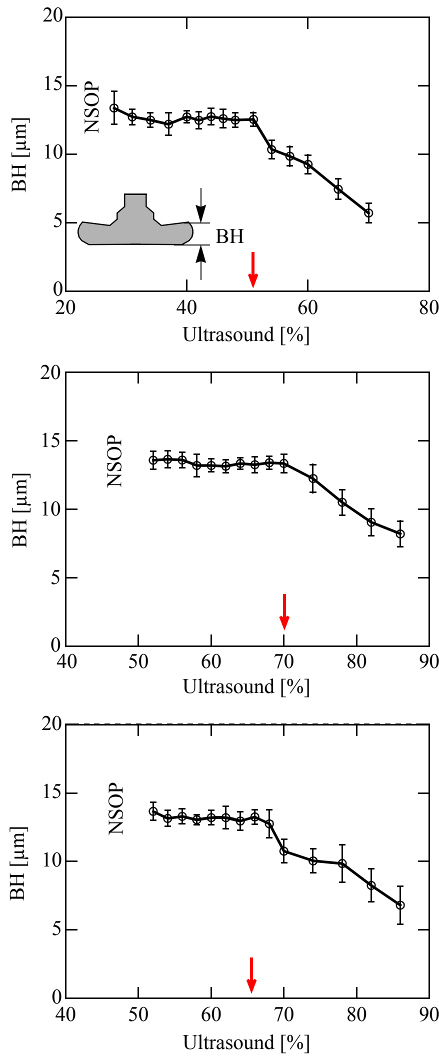

Fig. 8 Ball bond height vs. ultrasound for (a) Au, (b) Cu-H and (c) Cu-S wires.

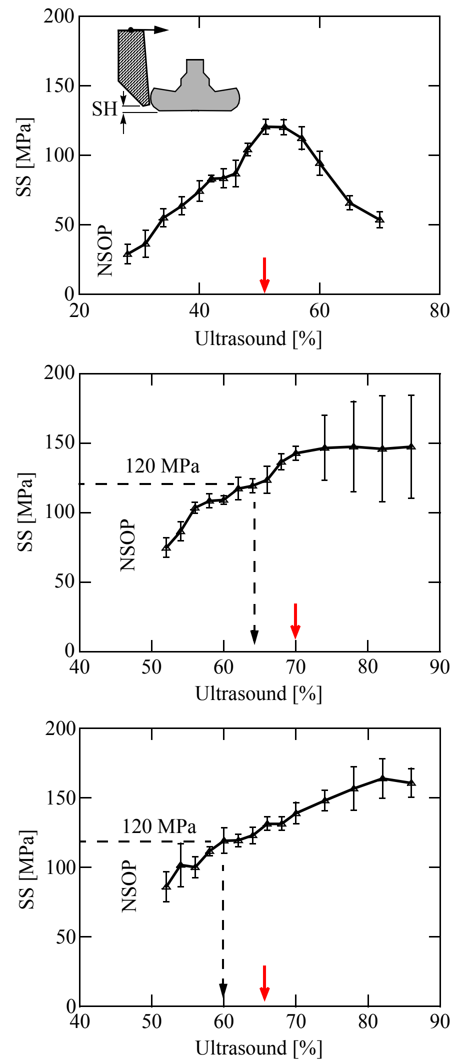

Fig. 9 Ball bond shear strength vs. ultrasound for (a) Au, (b) Cu-H and (c) Cu-S wires. ['SH' denotes shear height].

For the Cu ball bonding processes, the ultrasound level is reduced from the optimum value to a level at which we obtain a shear strength equivalent that is reached with Au ball bonding (120 MPa). In case of Cu-H wire, the ultrasound is reduced to 66% and for Cu-S wire, it is reduced to 60%, as indicated by the dashed arrows in Figs. 9 (b), and (c), respectively. While this causes the average shear strength to fall by about 15%, the c_{pk} does not change significantly, suggesting that a successful Cu ball bonding operation can be run at about 7-9% lower than the conventionally optimized value.

Microsensor calibration

To investigate the actual reduction of stress induced to the pad during the bonding process, ball bonding (for the optimized and reduced ultrasound settings as specified in Table 5) is performed on a special microsensor test chip designed by the Microjoining Laboratory of the University of Waterloo, Ontario, Canada. The microsensor test chip shown in Figs. 11 (a) and (b) contains thirteen bonding pads with integrated microsensors, connected to a bus by high temperature switches, and selectively sensitive to forces in y direction. The multiplexer is composed of a switch matrix

Table 5: Ultrasound settings for optimized and reduced process

Wire type	Optimized	Reduced
Au	51%	-
Cu-H	70%	64%
Cu-S	66%	60%

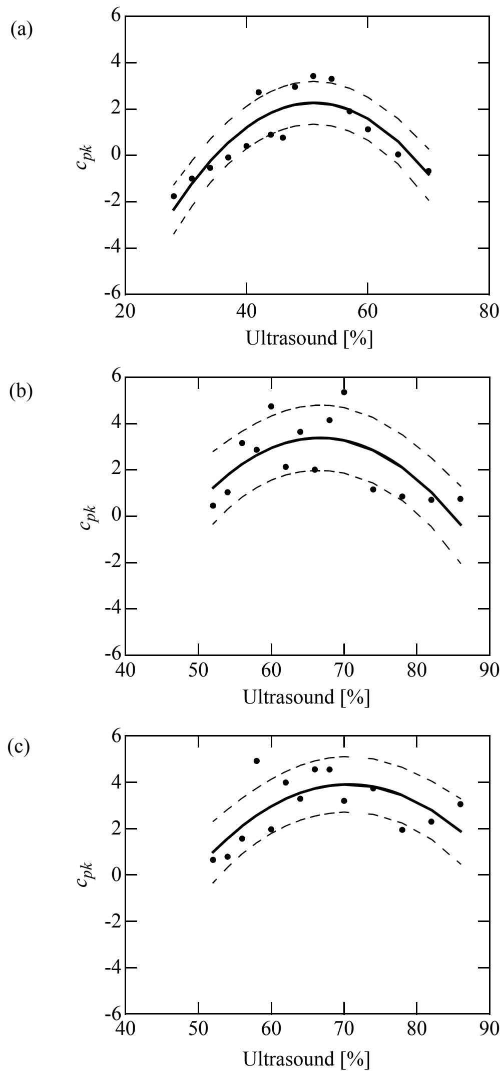

Fig. 10 Shear strength cpk values with a parabolic fit (dashed lines indicate ±1 standard deviation) vs. ultrasound for (a) Au, (b) Cu-H, and Cu-S wires.

and a 4-bit decoder. The principle, design, and operation of similar microsensors are described in detail in [9].

The microsensor is calibrated using the ESEC microsensor which was calibrated previously in Ref. [9]. The ESEC microsensor was provided by Oerlikon ESEC, Cham, Switzerland. To calibrate the microsensor, ball bonding tests are performed using a 50 µm Au FAB using a special ball bond program as shown in Table 6. The tests are performed at room temperature. As the ultrasound levels selected are lower than those required for bonding, the deformed FAB does not stick to the pad, and is subsequently bonded during the wedge bonding process. For the next test, a fresh FAB is fired. The tests are repeated for five samples of both types of microsensors. The results are compared and plotted in Fig. 12. From the plot, the calibration factor of the microsensor is determined to be 15.5 ± 0.9 mV/V/N.

Maximum Values of Ultrasonic forces

The microsensor chip is mounted on a gold plated polyimide substrate supplied by Oerlikon ESEC, Cham, Switzerland, using a commercially available adhesive. The

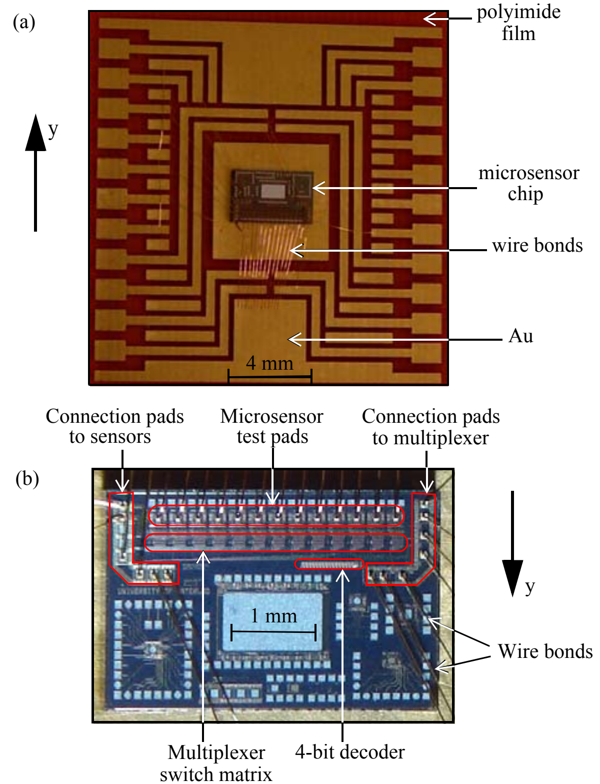

Fig. 11 (a) Microsensor test chip attached on gold metallization of polyimide substrate, (b) close-up of chip. Ultrasound in ± y direction for bonding tests.

Table 6: Bonding parameters for calibration experiment

Segment	Time [ms]	Force end [mN]	Ultrasound [%]
Impact Segment 1	1	800	-
Impact Segment 2	1	266	-
Bond Segment 1	5.3	266	3
Bond Segment 2	5.3	266	6
Bond Segment 3	5.3	266	9
Bond Segment 4	5.3	266	12
Bond Segment 5	5.3	266	15
Bond Segment 6	5.3	266	18
Bond Segment 7	5.3	266	21
Bond Segment 8	5.3	266	24

sensor channels and the multiplexer addressing channels are connected to the terminals on the substrate by gold wire bonds as shown in Fig. 11 (a). The measurement system is provided by Esec and described in [9]. A DC voltage of 3V is applied to the sensor.

Ball bonding using the optimized and reduced (for Cu-H and Cu-S wires) ultrasound level (shown in Table 5) is performed on the test pads with each of the three wire types, and the real time signals of the microsensor are recorded on a PC. The measurements are performed on 10 chips. For each setting listed in Table 5, the measurements are repeated 10 times. An example bond on the octagonal shaped bond pad of the microsensor is shown by the SEM micrograph in Fig. 13. Example signals for each of these five measurements along with their respective fundamental components are shown in Fig. 14.

The maximum ultrasonic force induced to the pad during the bonding process is evaluated at the point S shown in Fig. 14. The maximum ultrasonic force measured for optimum

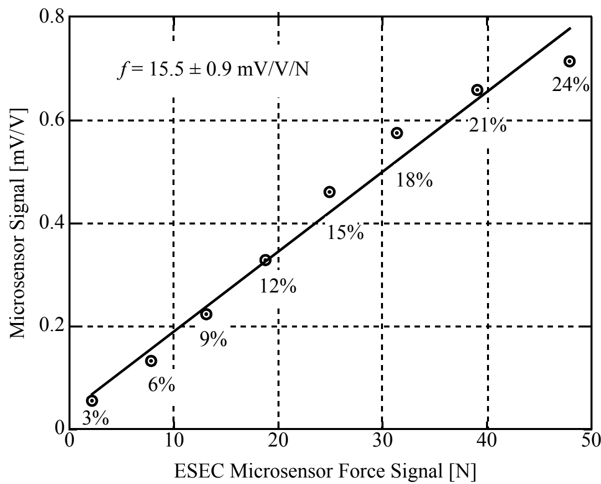

Fig. 12 Calibration of the microsensor using ESEC microsensor. The numbers below the markers indicate the ultrasound power in%.

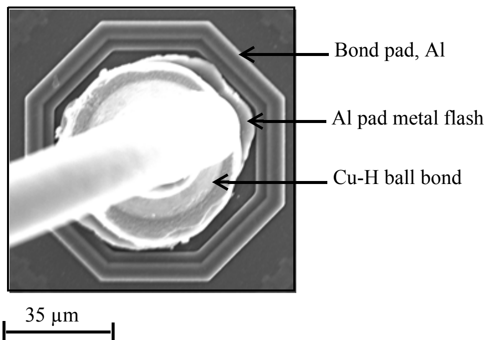

Fig. 13 SEM micrograph of Cu-H ball bond on the microsensor bond pad.

and reduced ball bonding processes with Au, Cu-H, and Cu-S wires are plotted in Fig. 15.

It is observed that the maximum ultrasonic force measured during optimized Cu ball bonding process is approximately

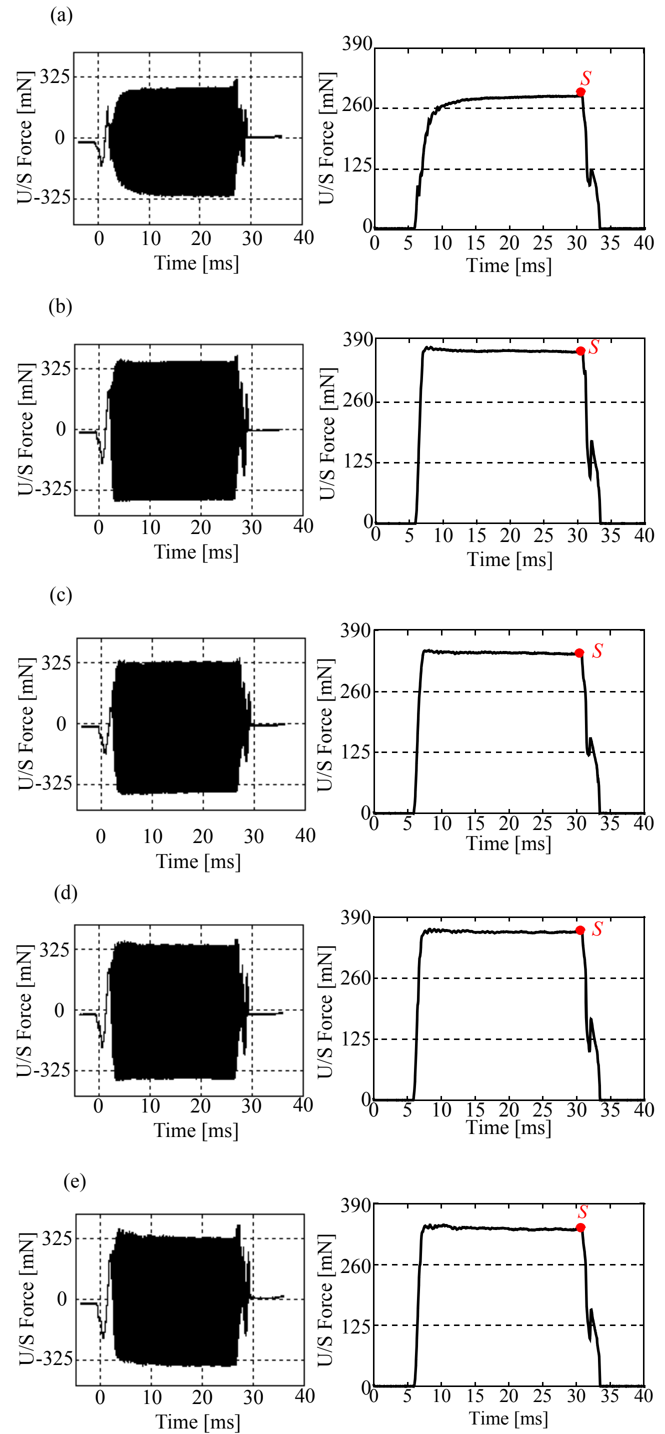

Fig. 14 Examples of ultrasonic force signals measured by the microsensor during ball bonding processes. Left: signals as measured. Right: signals conditioned for fundamental amplitudes. (a) optimized Au, (b) optimized Cu-H, (c) reduced Cu-H, (d) optimized Cu-S, (e) reduced Cu-S.

28-33% higher than that measured for optimized Au ball bonding process. It is observed that by using the softer of the two Cu wires (Cu-S), a stress reduction of about 5% is achieved. By using the reduced ultrasound process for the Cu-H and Cu-S wires, the bonding stress is reduced by approximately 9%. The reduced ultrasound Cu-S wire process succeeds in diminishing the force/stress gap to the Au wire process by 39%. Possibly the gap can be reduced further or even closed completely by using even softer wires than Cu-S and/or find a better impact force to bond force (IF/BF) ratio [10]. The IF/BF ratio used here is relatively high, resulting in considerable strain hardening of the Cu balls in particular. A low IF/BF ratio will result in softer bonded Cu balls, and less stress delivered to the chip during the process.

Conclusions

1. The Cu ball bonds show approximately 15% higher shear strength than the Au ball bonds. However, the ultrasonic stress measured by the integrated, real-time microsensors is about 30% higher for the Cu ball bonding process than for the Au ball bonding process.
2. The ultrasonic force measured for the softer Cu-S wire is about 5% lower than that measured for the harder Cu-H wire.
3. The new method to optimize the ball bond process parameters for Cu wires helps reducing the extra stress usually observed with Cu wire compared to that observed with Au wire by 39%.

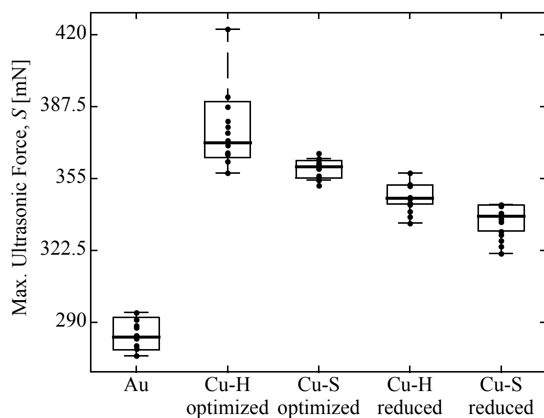

Fig. 15 Maximum ultrasonic stress for conventionally optimized process and reduced ultrasound process with Au, Cu-H and Cu-S wires.

Acknowledgements

The work is supported in part by Ontario Centers of Excellence (OCE), Natural Sciences and Engineering Research Council of Canada (NSERC), Microbonds Inc. (Markham, Ontario, Canada), and MK Electron Co. Ltd. (Yongin, Korea). Generous technical help of Oerlikon Esec is gratefully acknowledged.

References

1. Gaul, H. *et al*, “Predicting the Shear Strength of a Wire Bond using Laser Vibration Measurements”, *Proc of 1st Electronic System Integration Conference*, Vol. 2, 1996, pp. 719-725.
2. McKenna, R. G., and Mahle, R. L., “High Impact Bonding to Improve Reliability of VLSI Die in Plastic Packages”, *Proceedings of the IEEE Electronics Components Conference*, 1989, pp. 424-427.
3. Toyozawa, K. *et al*, “Development of Copper Wire Bonding Application Technology”, *IEEE Transactions on Components, Hybrids, and Manufacturing Technology*, Vol. 13, No. 4, 1990, pp. 667-672.Hang, C. *et al*, “On-line Hardness Characterization of Novel 2-mil Copper Bonding Wires”, *Proc ASME InterPACK’07 Conf*, 2007.
4. Lee, J. *et al*, “Iterative Optimization of Tail Breaking Force of 1 mil Wire Thermosonic Ball Bonding Processes and the influence of Plasma Cleaning”, *Microelectronics Journal*, Vol. 38, 2007, pp. 842-847.
5. Srikanth, N. *et al*, “Critical Study of Thermosonic Copper Ball Bonding”, *Thin Solid Films*, Vol. 462-463, 2004, pp. 339-345.
6. *Metals Handbook, Vol. 2 - Properties and Selection: Nonferrous Alloys and Special Purpose Materials*, ASM International, 10th Ed., 1990.
7. Montgomery, D., *Introduction to Statistical Quality Control*, John Wiley and Sons, New York, 2004.
8. *Wire Bond Shear Test Method*, Electronics Industries Alliance/JEDEC Standard EIA/JESD22-B116, 1998, pp. 7-8.
9. Schwizer, J. *et al*, *Force Sensors for Microelectronic Packaging Applications*, Springer Science+Business Media, Series: Microtechnology and MEMS, ISBN: 3-540-22187-5, 2005.
10. Shah, A. *et al,* "In situ Ultrasonic Force Signals during Low-Temperature Thermosonic Copper Wire Bonding", *Microelectronic Engineering*, Under review.